Bioartificial Sponges for Auricular Cartilage Engineering

Marta Feula[1], Mario Milazzo[2], Giulia Giannone[3], Bahareh Azimi[4], Luisa Trombi[4], Ludovica Cacopardo[1], Stefania Moscato[5], Andrea Lazzeri[3], Arti Ahluwalia[1], Stefano Berrettini[6], Carlos Mota[7], and Serena Danti[1,2,3](✉)

[1] Research Center "E. Piaggio", University of Pisa, 56122 Pisa, Italy
serena.danti@unipi.it
[2] The BioRobotics Institute, Scuola Superiore Sant'Anna, 56025 Pontedera, PI, Italy
[3] Department of Civil and Industrial Engineering (DICI), University of Pisa, 56122 Pisa, Italy
[4] Research Unit of DICI-Pisa, Interuniversity Consortium for Materials Science and Technology (INSTM), 50121 Florence, Italy
[5] Department of Clinical and Experimental Medicine, University of Pisa, 56126 Pisa, Italy
[6] Department of Surgical, Medical, Molecular Pathology and Emergency Medicine, University of Pisa, 56126 Pisa, Italy
[7] Institute for Technology Inspired Regenerative Medicine (MERLN), Complex Tissue Regeneration Department, Maastricht University, 6229ER Maastricht, The Netherlands

Abstract. Auricle reconstruction due to congenital, post-infective or post-traumatic defects represents a challenging procedure in the field of aesthetic and reconstructive surgery due to the highly complex three-dimensional anatomy of the outer ear. Tissue engineering aims to provide alternatives to overcome the shortcomings of standard surgical reconstructive procedure. In the present study, poly(vinyl alcohol)/gelatin (PVA/G) sponges at different weight ratios were produced via emulsion and freeze-drying, and crosslinked by exposure to glutaraldehyde vapors. PVA/G sponges gave rise to highly porous, water stable and hydrophilic scaffolds. Characterization of PVA/G sponges showed round-shaped interconnected pores, high swelling capacity (>200%) and viscoelastic mechanical behavior. The PVA/G 70/30 (w/w) scaffold was selected for *in vitro* biological studies. Bone marrow derived human mesenchymal stromal cells (hMSCs) were used and differentiated towards chondrogenic lineage under different culture conditions: *1)* commercial versus handmade differentiation medium; *2)* undifferentiated versus pre-differentiated hMSC seeding; and *3)* static versus dynamic culture [i.e. ultrasound (US) or bioreactor stimulation]. Histological results highlighted intense glycosaminoglycan, glycoprotein and collagen syntheses after three weeks, mostly using the commercial medium, whereas round morphology was observed in pre-differentiated cells. In static culture, immunohistochemistry for chondrogenic markers revealed an early differentiation stage, characterized by the expression of Sox-9 and collagen type I fibers. The application of US on cell/scaffold constructs increased extracellular matrix deposition and resulted in

S. Piotto et al. (Eds.): BIONAM 2019, LNBE, pp. 191–209, 2020.
https://doi.org/10.1007/978-3-030-47705-9_17

30% higher collagen type II expression at the gene level. Bioreactor culture induced collagen type II, aggrecan and elastin formation. This study demonstrated that 70/30 PVA/G sponge is a suitable candidate for auricle reconstruction.

Keywords: Auricle · Tissue engineering · Mesenchymal Stromal Cells · Poly (vinyl alcohol) (PVA) · Emulsion

1 Introduction

Auricle malformation or absence due to congenital or acquired defects represents a relevant clinical problem, since it also negatively affects patient's psychological well-being. Surgical auricle reconstruction represents one of the most challenging procedure in the field of aesthetic and reconstructive surgery due to the highly complex three-dimensional anatomy of the external ear [1, 2]. Current surgical treatments include the use of rib cartilage autograft and alloplastic biomaterials for auricle reconstruction [1, 3, 4]. The application of a prosthetic auricle has been investigated as an alternative to surgical reconstruction, since it provides good aesthetic results minimizing risks associated with the surgical procedure [5]. The main shortcomings associated to the aforementioned treatments are related to surgical complications and foreign body reaction; therefore, scientists are investigating tissue engineering techniques to regenerate auricle cartilage in vitro [3, 4, 6]. In 1997, Cao *et al.* generated the first ear-shaped cartilage construct in an animal model [7], thus disclosing tissue engineering potential in auricle reconstruction. Since then, many researchers have focused their attention on the possibility of engineering the human auricle. The first successful results were obtained by employing a multistep approach: in the first step, chondrocytes were seeded on a polymeric ear-shaped scaffold; then, cell/scaffold construct was implanted in an animal at subcutaneous level; successively, the regenerated cartilage was harvested, manipulated and re-implanted in patients [1, 8]. Recently one of the most investigated option is the combination of computer tomography (CT) scan and additive manufacturing technologies to fabricate patient-specific ear-shaped scaffolds in order to regenerate cartilage constructs *in vitro* [3, 9].

The auricle, the external auditory meatus and the Eustachian tube consist of elastic cartilage [6, 10]. The properties of auricular cartilage depend on characteristics and spatial distribution of its main structural components: collagen fibers, elastic fibers, glycosaminoglycans (GAGs), chondrocytes and water [11–13]. Chondrocytes are round-shaped and can be observed as single cells or isogenic groups composed by two or three cells surrounded by abundant extracellular matrix (ECM) [10, 14]. In the ear, collagen fibers mainly consist of collagen type II, which are responsible for tensile strength, while elasticity and flexibility of the tissue are due to the presence of elastic fibers, peculiar to elastic cartilage [15, 16]. On the other hand, GAGs possess negatively charged sulfate groups able to attract water molecules and bind proteoglycans to collagen fibrils, thus providing unique biomechanical properties and a viscoelastic component [17]. Cartilage predominant proteoglycan is aggrecan, which provides cartilage elasticity and viscosity retention [18]. In addition, the elastic cartilage ECM contains smaller proteoglycans such as biglycan, decorin and fibromodulin, glycoproteins as fibronectin and other non-collagenous proteins [13].

Auricular cartilage, as any other biological tissue, shows viscoelastic behavior. As such, elastin biomechanically behaves as a linear elastic solid and can be elastically deformed up to 160% strain values [19]. The stress-strain curve obtained by mechanical testing of elastin samples is essentially linear, even though there is a slight difference between loading and unloading curve due to a phenomenon of energy dissipation within the material [19]. Elastin elasticity is a direct consequence of the entropic recoil of elastin molecules [20]. Collagen is a basilar structural protein able to provide mechanical integrity and strength to soft tissues, thus playing a key role in determining tissue biomechanical properties [19, 21].

Data dealing with auricular cartilage mechanical properties available in literature are limited. Griffin *et al.* tested samples of human auricular cartilage harvested from cadavers (average age 69 $\pm$ 10 years) in order to explore the biomechanical properties of this tissue [4]. Compressive test reported an overall elastic modulus of 1.66 $\pm$ 0.63 MPa without significant differences among the different anatomical regions in which human auricle can be divided [4]. Elastic cartilage does not undergo calcification; however, its biomechanical properties change as a consequence of ageing [10, 14]. Individual's age advancing is related to significant changes in matrix thickness and composition: the amount of elastin decreases, elastic fibers are thinner and more fragmented, chondrocytes number and size drop [22–24]. These changes progressively compromise cartilage mechanical integrity [23, 25].

Studies conducted in the nineties have demonstrated that both bovine chondrocytes and human chondrocytes are able to replicate and generate cartilage matrix when seeded on synthetic scaffolds [25, 26]. However chondrocytes isolated from articular, costal or septal cartilage are not able to synthesize elastin, thus regenerated tissues show fibrocartilaginous nature and present lower biochemical and mechanical properties than native elastic cartilage [3, 27]. Nevertheless, only a small amount of tissue can be harvested from the patient, thus an extensive *in vitro* expansion of chondrocytes is required in order to obtain a sufficient number of cells to produce cartilage engineered constructs of clinically relevant size [27]. Furthermore, chondrocyte proliferative potential is physiologically low and their capability to produce cartilage matrix decline over time [27].

Therefore, to allow the regeneration of such specific ECM, it is fundamental to provide a suitable scaffold in which chondrogenesis and elastic cartilage formation can take places. It is well known that once chondrocytes are cultured on tissue culture plastic, namely, in a bidimensional (2D) setting, they lose their morphotype, from round to spindle-like, and finally de-differentiate into fibroblasts, which in turn produce different ECM molecules, including a prevalence of collagen type I [27]. Differently, a tridimensional (3D) setting is considered the best option to obtain a cartilaginous tissue *in vitro*.

Previous studies have already proved that bone marrow derived mesenchymal stromal cells (MSCs) are able to differentiate into chondrocytes and express chondrogenic markers, such as aggrecan and collagen type II when adequately stimulated [28, 29]. The employment of MSCs for *in vitro* cartilage engineering presents several benefits as a low number of cells is initially required and their isolation from bone marrow is relatively easy and already adopted in clinical procedures [6]. However, prolonged *in vitro* cultivation is necessary in order to obtain noticeable chondrogenic

differentiation. MSCs are not involved in the physiological development of auricular cartilage and so far there is no evidence that elastic fibers can be obtained [27, 30]. To induce the regeneration of auricular cartilage, suitable chemical and physical signals should be provided. Chemical signals can be introduced in the scaffold by blending synthetic with biological polymers [31–35], and MSCs can be activated towards chondrogenic cascade by using proper supplements in the culture medium [3, 6, 29, 35, 36]. Dynamic stimuli, such as low intensity ultrasound (US) stimulation, have been reported to promote chondrogenic marker expression and can be applied to the cell/scaffold constructs during the culture [18, 35, 37–39].

The aim of this study is the fabrication and characterization of a bioartificial scaffold for auricular cartilage engineering. Specifically, poly(vinyl alcohol) (PVA), a biocompatible synthetic polymer was blended with gelatin (G) and additionally combined Alginate (Alg) to produce hydrophilic sponges able to emulate native ECM and facilitate cell adhesion. Human MSCs (hMSCs) from the bone marrow were used as a cell source since they can be easily isolated from bone marrow and are able to extensively replicate *in vitro* and differentiate in chondrocytes. As chondrogenic differentiation can be enhanced by the application of dynamic stimulation, low frequency US was applied, and a pilot study in a bioreactor was also performed. Specific objectives of the study are the identification of the optimal scaffold composition and the assessment of the optimal hMSC differentiation protocol.

2 Materials and Methods

2.1 Sponge Fabrication

PVA-based scaffolds were produced via emulsion and freeze-drying, as detailly described by Ricci & Danti [40]. A 11.7% aqueous solution of PVA (Mw = 89000–98000 g/mol, >99% hydrolyzed from Sigma-Aldrich, St. Louis, MO, USA) in Milli-Q® deionized water (to avoid Ca^{2+} ions contamination, thus unwanted sodium Alginate crosslinking during emulsification) was autoclaved 1 h at 120 °C and then was cooled down to 50 °C inside a thermostatic bath under stirring at 1000 rpm. Gelatin (gelatin from bovine skin, type B, from Sigma-Aldrich) and Alginic acid sodium salt (Alg; Fluka BioChemika) were added in order to obtain different polymer/biomolecule composition: PVA/G 90/10, 80/20, 70/30 and PVA/G/Alg 80/10/10 and 90/5/5 (w/w)%. Then, 0.18 g of sodium dodecyl sulfate (SDS; from Sigma-Aldrich) were added to obtain a dense foam. After 10 min under stirring, the foam was poured into a six-well plate, quenched in liquid nitrogen and lyophilized. Sponges were crosslinked by exposure to glutaraldehyde (GTA; grade II, from Sigma-Aldrich) vapors for 72 h at 37 °C in a sealed cabinet and then flushed under the chemical hood for 72 h.

2.2 Scaffold Characterization

Scanning Electron Microscopy (SEM) Analysis

PVA/G samples 90/10, 80/20 and 70/30 (w/w)% were mounted on aluminum stumps, sputter-coated with gold (Sputter Coater Emitech K550, Quorum Technologies Ltd,

West Sussex, United Kingdom) and examined on a scanning electron microscope (JEOL JSM-5200, JEOL Ltd, Tokyo, Japan). Approximative pore size distribution was evaluated using ImageJ software (version 1.51i, NIH, USA).

Swelling Analysis

Swelling analysis was performed by measuring sample volume before and after swelling in distilled water at different time points. Volume swelling ratio (Q, Eq. 1) was calculated according to the following equation:

$$Q = \frac{\text{Volume of hydrated sample}}{\text{Volume of dry sample}} \times 100 \quad (1)$$

Differential Scanning Calorimetry (DSC) Analysis

Phase transition properties of the samples were determined using a DSC Q200 Differential Scanning Calorimeter controlled by a TA module (TA Instruments, New Castle, USA). 7–8 mg of dry samples were placed in hermetically sealed aluminum pans and heated from −35 °C to +250 °C at a heating rate of 10 °C/min in an inert atmosphere. An empty pan was used as the reference cell. Transition temperatures were calculated using the Universal Analysis 2000 software (TA Instruments).

Fourier Transformed Infrared Spectroscopy (FTIR) Analysis

FTIR spectra were recorded using Nicolet 380 FT-IR Spectrometer (ThermoFisher Scientific, USA) equipped with the Thermo Scientific™ Smart™ iTX accessory. The spectra were recorded between 4000 cm^{-1} and 550 cm^{-1} with a 8 cm^{-1} spectral resolution. For each spectrum 256 scans were co-added. The FTIR spectrum was taken in a transmittance mode. Data were analyzed using EZ OMNIC Software (ThermoFisher Scientific, USA).

Gelatin Release Evaluation

Gelatin release from crosslinked and non-crosslinked PVA/G sponges was evaluated by means of a spectrophotometric method. Briefly, 5 mg of PVA/G sponges at different (w/w)% composition were immersed in 1 ml of phosphate buffer saline (PBS) and incubated at 37 °C for 96 h. Then, released solution was collected from each sample, diluted in PBS and 200 μL of Bradford reagent (Bio-Rad, USA) were added. The absorbance of the solution at 595 nm was measured using a photometer (BioPhotometer plus, Eppendorf, Germany). Gelatin concentration in the release solution was determined through comparison with a calibration curve.

Mechanical Testing

Viscoelastic properties of PVA/G sponges at different (w/w)% ratios were investigated by using epsilon dot method [41, 42]. Mechanical tests were performed in triplicate on hydrated samples. Short compressive tests were performed at different strain rates (0.005, 0.001, 0.0005 s^{-1}) using the twin column ProLine Z005 testing machine (Zwick Roell) equipped with a 10 N load cell (Zwick KAP-TC). Force and displacement data were recorded over time (sampling rate 1 kHz). Firstly, data were processed to obtain stress-time series. Apparent elastic moduli were calculated as the slope of stress-strain curves and linear viscoelastic region (LVR) was identified. A standard linear solid (SLS) model was chosen to derive PVA/G viscoelastic parameters.

Viscoelastic parameters, i.e. the instantaneous (E_{inst}) and equilibrium elastic moduli (E_{eq}) and the characteristic relaxation time (τ), were estimated by globally fitting stress-time series in a combined parameter space using OriginLab (Northampton) fitting toolbox [41, 42].

2.3 Biological Study Design

PVA/G 70/30 (w/w)% sponges were cut in cylindrical scaffolds (5 mm in diameter and 1.5 mm in thickness) using a biopsy puncher and a microtome blade. Scaffolds were sterilized in absolute ethanol (Bio-Optica, Milan, Italy) for 24 h and then treated with 2% glycine (Sigma-Aldrich) for 1 h in order to block unreacted sites of GTA. Therefore, scaffolds were washed three times in PBS supplemented with antibiotics.

Study Design

Human mesenchymal stromal cells (hMSCs) (Merk, Germany) were defrosted and expanded according to the manufacturer's recommendations. HMSCs at passage 2 were trypsinized, seeded on PVA/G 70/30 scaffolds (puncher cut into 5 mm in diameter and 1.5 mm in thickness) at a density of 500,000 cell/scaffold and differentiated for 21 days in standard culture conditions, namely, 95% air, 5% CO_2 in humidified incubator at 37 °C. At the endpoint samples were processed for metabolic activity tests, SEM and histological analyses. If not otherwise specified, all reagents were purchased from Sigma–Aldrich.

The following culture conditions were applied: *1)* commercially available chondrogenic differentiative medium *versus* homemade culture medium; *2)* seeding undifferentiated *versus* pre-differentiated hMSC; *3)* static *versus* dynamic cultures. Specifically:

1) Cells were seeded on PVA/G 70/30. After 1 day the culture medium was replaced with chondrogenic differentiative media. Two chondrogenic differentiation media were used:

1a) StemMACS ChondroDiff medium was purchased from Miltenyi Biotec (Bergisch Gladbach, Germany).

1b) Homemade chondrogenic medium was obtained as reported by Barachini *et al.* [43]. Briefly, homemade chondrogenic medium consisted of DMEM/F12, 1.25 μg/ml bovine serum albumin, 5.35 μg/ml linoleic acid, 50 μg/ml ascorbic acid, 100 μg/ml sodium pyruvate, insulin–transferrin–selenium (ITS premix), 10^{-7} M dexamethasone and 10 ng/ml transforming growth factor beta 1 (TGF-β1; PeproTech, Rocky Hill, NJ).

2) Two pre-differentiation strategies were considered:

2a) Pre-differentiation in pellet conditions as described by Barachini *et al.* [43]. Briefly, 250,000 hMSCs/tube, were centrifuged at 1200 rpm for 7 min to obtain chondrogenic pellets, which were washed in sterile saline and cultured in chondrogenic medium StemMACS Chondrodiff medium (Miltenyi). Pellets were cultured 1 week in Milteniy ChondroDiff medium, then trypsinized, seeded on PVA/G 70/30 scaffolds and differentiated for more 14 days.

2b) Pre-differentiation in 2D conditions on tissue culture plastic flasks for 4 days, as reported by Bajpai *et al.*, by adding StemMACS ChondroDiff (Miltenyi) medium

[44]. After the pre-differentiation in 2D conditions, the cells were trypsinized, seeded on PVA/G 70/30 scaffolds and differentiated for ~~more~~ further 17 days.

3) Dynamic stimulations:

3a) Cell/scaffold constructs were daily treated 3 times for 5 s with US at 40 kHz frequency and 20 W power in a sonicator bath (Bransonic 2510; Bransonic, Danbury, USA) as reported by Barachini *et al.* [43]. After 1 day the culture medium was replaced with chondrogenic differentiative media: Milteniy ChondroDiff medium was added to a set of samples ($n = 3$) as in *1a)* and the home-made chondrogenic medium was added to the other set ($n = 3$) as in *1b)*. Cells were differentiated for 21 days.
In addition, hMSCs, pre-differentiated in 2D conditions as in *2b)*, were seeded on PVA/G 70/30 scaffolds ($n = 8$) and differentiated for 21 days. A set of samples ($n = 4$) was daily treated with US three times for 10 s each time, while the other set ($n = 4$) served as negative control.

3b) In a pilot study, pre-differentiasted hMSCs as in *2b),* were trypsinized and seeded on a PVA/G 70/30 (w/w)% scaffold (25 mm in diameter and 1 mm in thickness to fit the bioreactor holder) at a density of 800,000 cells/scaffold and then cultured in StemMACS Chondrodiff medium (Miltenyi) into a patented bioreactor (WO/2015/040554) which moved the construct at 0.23 Hz for 15 min every 30 min rest intervals for 14 days.

2.4 Biological Analysis

Cell metabolic activity

AlamarBlue® assay was performed once a week in order to assess cell viability. Cell/scaffold constructs to be tested were placed in 15 ml Falcon tubes and alamarBlue® reagent (Life Technologies, USA) was added, according to manufacturer's prescriptions. AlamarBlue solution without cells served as negative controls. After 3 h of incubation, 100 µl samples were collected in triplicate and analyzed with a plate reader (Victor3, PerkinElmer, Waltham, USA). Absorbance values at 570 nm and 600 nm were recorded and used to calculate dye reduction percentage. At the end of the test, fresh culture medium was added.

Histological Analysis

Cell/scaffold constructs were fixed in 4% w/v neutral buffered formalin diluted in 1× PBS (0.1 M, pH 7.2) (Bio-Optica) overnight at 4 °C. Thereafter samples were washed in PBS, dehydrated with a graded series of ethanol, clarified in xylene and finally paraffin-embedded. Finally, 8 µm-thick sections were obtained by standard microtomy and mounted onto glass slides and stained with hematoxylin-eosin (H&E), Alcian Blue at pH 1 and pH 2.5, Toluidine Blue, orcein-Van Gieson; periodic acid-Schiff (PAS) reaction was also performed.

Immunohistochemical analysis was carried out on cell/scaffold constructs, by following a standard protocol described in details by Barachini *et al.* [43]. The following antibodies with specified concentrations were used: mouse monoclonal anti-human elastin 1:50 (AB9519, AbCam, Cambridge, United Kingdom); rabbit polyclonal anti-human type I collagen 1:1000 (AB34710, AbCam); mouse monoclonal anti-human

aggrecan 1:50 (SC33695, Santa Cruz Biotechnology, USA); rabbit polyclonal anti-human Sox9 1:100 (SC20095, Santa Cruz Biotechnology); mouse monoclonal anti-human type II collagen 1:50 (SC52658, Santa Cruz Biotechnology). All the histological analysis were observed with a Nikon Eclipse Ci microscope (Nikon Instruments, Amsterdam, The Netherlands) and the images were acquired by a digital camera equipped on the microscope.

Gene Expression

Real time polymerase chain reaction (RT-PCR) was performed in order to investigate type II collagen gene expression on US-irradiated and non-US irradiated cell/scaffold constructs. Total RNA was isolated with Tri reagent® (Sigma-Aldrich) and 500 ng of this were reverse-transcribed into complementary DNA (cDNA) using M-MLV-Reverse transcriptase (Promega), at 37 °C for 45 min, according to the manufacturer's instructions. RT-PCR for quantification of expression levels human Collagen-2 was carried out with the LC Fast Start DNA Master SYBR Green kit (Roche) using 2 μl of cDNA, corresponding to 500 pg of total RNA in a 20 μl final volume, 3 mM $MgCl_2$ and 0.5 μM sense primer (5'-CAACACTGCCAACGTCCAGAT-3') and antisense primer (5'- CTGCTTCGTCCAGATAGGCAA-3'), using β-actin as housekeeping gene (5'-GACGACGACAAGATAGCCTAGCAGCTATGAGGATC-3' and 5'- GAG GAGAAGCCCGGTTAACTTCCGCAGCATTTTGCGCCA3'). Melting curves were generated after each run to confirm the amplification of specific transcripts. Reactions were carried out in duplicate, and the relative expression of a specific mRNA was determined by calculating the fold change relative to the β-actin control. The fold change of the tested gene mRNA was obtained with a LightCycler® software, by using the amplification efficiency of each primer, as calculated by the dilution curve. The specificity of the amplification products was verified by subjecting the amplification products to electrophoresis on 1.5% agarose gel and visualization by ethidium bromide staining (Sigma Aldrich).

2.5 Statistical Analysis

One-way analysis of variance with post-hoc Tukey's test was performed using OriginLab (Northampton). Statistical significance was assumed at a value of $p < 0.05$. Data are reported as mean ± standard deviation.

3 Results and Discussion

3.1 Sponge Characterization

Morphological Characterization

The mixture of a biocompatible and hydrophilic synthetic polymer, such as PVA, and natural polymers, such as protein and polysaccharide components (i.e., bioartificial material) was considered in order to mimic a preliminary ECM. The PVA/G/Alg foam collapsed after freeze-drying. Similar results in terms of structure collapse and shrinkage were observed by Gurikov *et al.* [45]. Vice versa, PVA/G sponges gave rise

to highly porous, water stable and hydrophilic scaffolds, which were selected for further characterization (Fig. 1) [33, 40, 43].

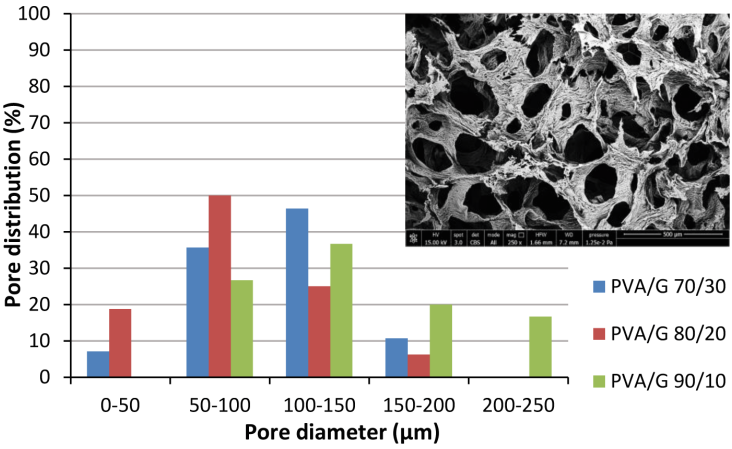

Fig. 1. Pore diameter distribution of PVA/G sponges at different (w/w)%. Lens shows a typical section of PVA/G sponge with round and interconnected pores.

The morphology of the PVA/G sponges was analyzed via SEM to assess pore interconnectivity. SEM analysis confirmed the porous nature of the sponges, highlighting round shaped interconnected pores with diameters ranging in 50–250 µm (Fig. 1), suitable to cell infiltration. Pore size distribution results, acquired via ImageJ, were in line with those observed by De la Ossa *et al.*, evaluated with mercury intrusion porosimetry [46].

Physico-Chemical Characterization

DSC thermograms showed the presence of two endothermal events. The first endothermal event, between 83 °C and 102 °C, was due to water evaporation. As reported by Chiellini *et al.*, the highly energetic water evaporation process may interfere with the detection of G endothermic relaxation, which typically occurs at about 91 °C in dried gelatin samples [47, 48]. Differences between crosslinked and non-crosslinked samples at these temperatures demonstrated that the latter sponge had a greater capability to interact with water. The second endothermal event was represented by a sharp peak at 226–230 °C, associated to the melting of PVA crystals. PVA crystals melting temperature observed in these blends was significantly higher than the melting temperature of about 191 °C found by Chiellini *et al.* and Alves *et al.* for pure PVA films [47, 49]. The increasing of melting temperature in PVA/G blends can be explained as a consequence of the intense interaction between G molecules and PVA, thus proving a good compatibility between the two components at different (w/w)% ratios [50]. The FTIR spectra obtained presented the typical peaks of PVA/G blends reported in previous works on the characterization of polymeric films for biomedical

applications [49–51]. In general, the complexity of the spectrum within material fingerprint region increased by increasing G content. A characteristic absorption peak at 1450 cm^{-1} demonstrated the formation of CH = N groups due to the reaction of GTA with -NH_2 groups of lysine residues [46]. The difference between crosslinked and non-crosslinked spectra became more pronounced by increasing G content, as previously reported by De la Ossa *et al.*, on PVA/G sponges [46]. There was no appreciable G release from all the crosslinked samples, thus proving sponge water stability at physiological temperature after chemical cross-linking with GTA. Swelling analysis is reported in Fig. 2.

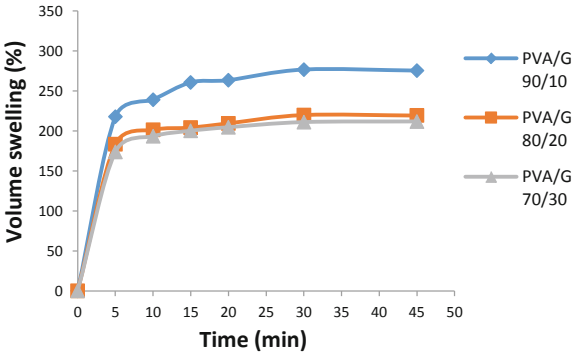

Fig. 2. Volume swelling ratio of PVA/G sponges at different G concentrations (90/10, 80/20, 70/30 w/w%).

It demonstrated the good capability of crosslinked sponges to interact with water, by acquiring a highly hydrated configuration. Samples quickly reached swelling equilibrium, presenting volume swelling ratio higher than 200%, thanks to the hydrophilic nature of PVA and G (Fig. 2). Volume swelling ratio decreased with increasing G content as a consequence of the dense network of crosslinks established after chemical crosslinking with GTA.

Mechanical Characterization

Experimental stress-time series within the LVR (2% strain) were used to estimate viscoelastic parameters, according to epsilon dot method. The sponges became less stiff (E_{eq} decreased) and more elastic and less liquid-like (τ increased) as the G content decreased (Table 1).

Table 1. PVA/G viscoelastic parameters derived from fitting of experimental data.

	PVA/G 70/30	PVA/G 80/20	PVA/G 90/10
E_{inst} [kPa]	6.85 ± 1.52	8.86 ± 1.42	2.12 ± 0.33
E_{eq} [kPa]	5.96 ± 1.53	6.79 ± 1.02	1.61 ± 0.50
τ [s]	1.34 ± 0.32	3.06 ± 3.70	9.29 ± 5.95
R^2	>0.99	>0.99	>0.99

The apparent elastic moduli of PVA/G samples, calculated as the slopes of stress-strain curves, are reported in Table 2. Slight variations with strain rate revealed that hydrated PVA/G sponges exhibited viscoelastic behavior. Moreover, G content $\geq$ 20% resulted in a significant increase in material stiffness. This phenomenon is likely to be a consequence of crosslinking. Indeed, the reaction of GTA aldehyde groups with free lysine or hydroxylysine residues of G polypeptide chains limits polymeric chain mobility by creating a network of crosslinks [48]. Statistical analysis underlined that PVA/G 90/10 presented a significantly lower elastic modulus, thus demonstrating that an increasing in G content and consequently, increasing of crosslinking sites, affected the material stiffness.

Table 2. Apparent compressive elastic modulus [kPa] of PVA/G sponges at different strain rates [s^{-1}].

Strain rate	PVA/G 70/30	PVA/G 80/20	PVA/G 90/10
0.005	6.61 ± 1.57	7.27 ± 0.23	2.03 ± 0.35
0.001	6.11 ± 1.60	7.25 ± 0.07	1.81 ± 0.49
0.0005	5.95 ± 1.46	7.09 ± 0.08	1.73 ± 0.53

Although the elastic moduli of PVA/G sponges was about three orders of magnitude lower than compressive elastic modulus of human auricular cartilage reported in literature [4, 23], an increase in construct stiffness is expected as a consequence of ECM deposition and in particular collagen synthesis within scaffold pores. The mechanical properties of cell/scaffold constructs after differentiation time were not tested because the small dimensions of the engineered constructs was not suitable for mechanical testing with the equipment available. To address this issue, further studies may include nanoindentation tests using the nano-epsilon dot method [52], which allows the investigation of viscoelastic parameters before and after cell culture. In addition, new devices which enable monitoring of the mechanical properties of tissue constructs during cell culture such as the Mechano Culture Testing System [53] could also be considered.

3.2 Characterization of Cell/Scaffold Constructs

The aforementioned characterization highlighted significant differences between PVA/G sponges in terms of pore size distribution, swelling behavior, physico-chemical and mechanical properties. PVA/G 70/30 and PVA/G 80/20 (w/w)% had more similar characteristics, namely, pore size distribution suitable for cell colonization, good swelling behavior and higher stiffness than PVA/G 90/10 (w/w)%. Finally, PVA/G 70/30 was selected as the best scaffold candidate, on the basis of stiffness, highest G content, which facilitates cell adhesion, and suitable poral features for cell colonization, as previously studied by De la Ossa *et al.* [46].

Chondrogenic Differentiation of hMSC/Scaffold Constructs
AlamarBlue assay, performed at different time points during chondrogenic differentiation, demonstrated that hMSCs cultured on PVA/G 70/30 scaffolds were viable up to three weeks in all tested samples (Fig. 3).

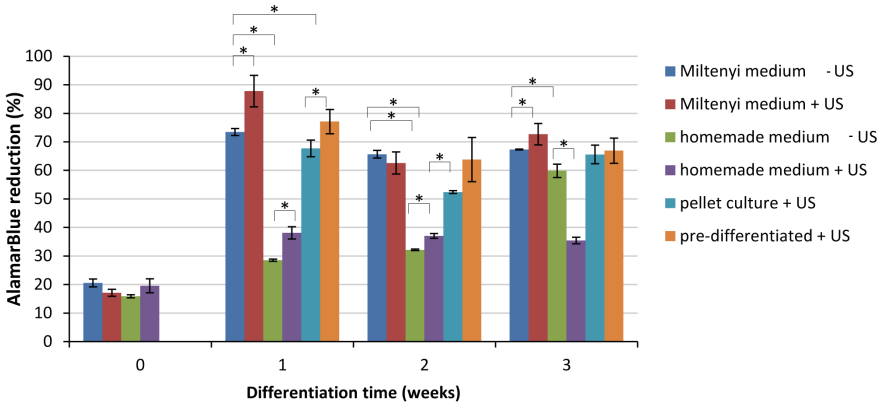

Fig. 3. Viability of chondroinduced hMSCs over differentiation time (0 week refers 12 h after seeding) in different culture conditions.

Miltenyi ChondroDiff medium was the best-performing differentiative medium. Indeed, significant lower cell metabolic activity was observed in constructs cultured in the homemade chondrogenic medium. Moreover, statistically significant differences between US-stimulated samples and negative controls demonstrated that US stimulation treatment affected cell metabolism. These results agree with the outcomes reported by Barachini *et al.* in their work on chondrogenic differentiation of human dental pulp stem cells on PVA/G 80/20 [43].

Histochemistry and Immunohistochemistry
In agreement with the metabolic activity results (Fig. 3), the scaffolds hosted varying amounts of cells, as observed via H&E staining. High positivity for Sox9 chondrogenic marker, observed in all tested samples, indicated an early differentiation stage of all the constructs (data not shown). A meaningful representation of the results achieved in the different conditions in terms of ECM maturity is reported in Fig. 4. Cell/scaffold constructs cultured in homemade chondrogenic medium displayed low glycoprotein, GAG (Fig. 4 C, D) and collagen (Fig. 4 I, J) expression and a non-uniform cell colonization. Conversely, a good and uniform cell spreading was detected in all samples cultured in Miltenyi StemMACS ChondroDiff medium (Fig. 4 A, B, E, F, G, H, K, L). Intense GAG deposition and roundish morphology was observed in hMSCs pre-differentiated in pellet conditions; however, cell colonization was restricted to a small region of the scaffold since the pelletized cells remained locally confined, thus providing no physiologically relevant results. HMSCs cultured in Miltenyi StemMACS ChondroDiff medium showed very good amount of collagen (Fig. 4 A, B, E, F) and GAGs (Fig. 4 G, H, K, L), as well as glycoproteins (data not shown).

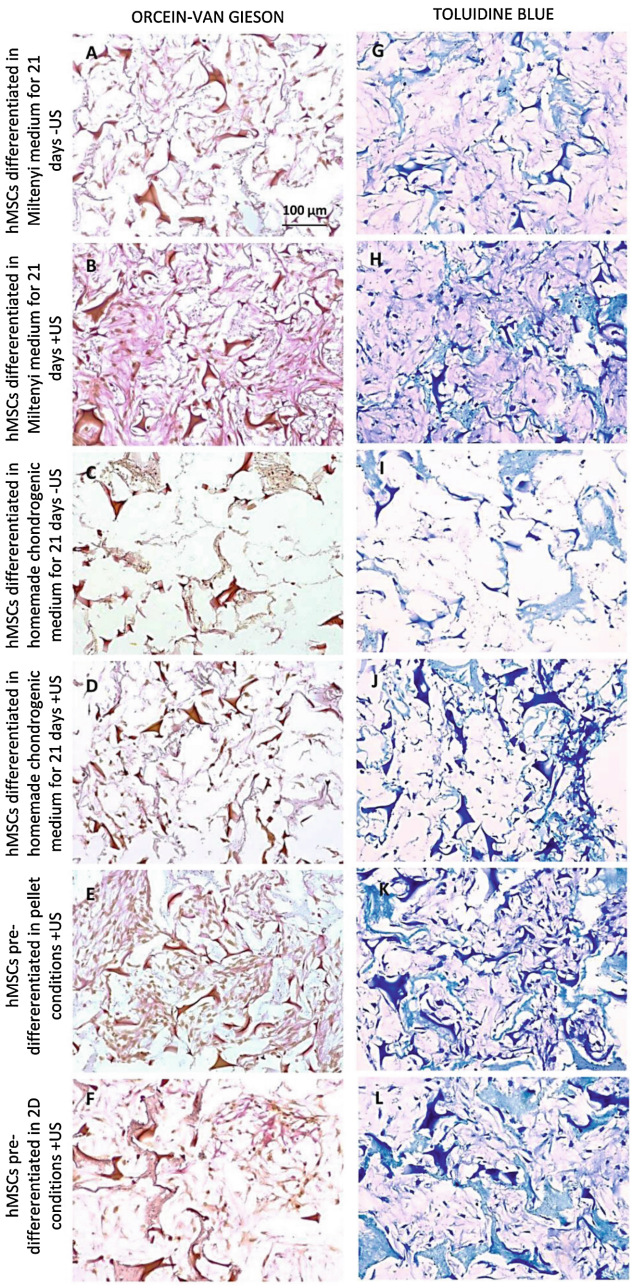

Fig. 4. Chondroinduced hMSCs cultured on PVA/G 70/30 scaffolds. Left column: Orcein-van Gieson staining: Orcein highlights the presence of elastic fibers in dark violet (absent in our samples). Van Gieson stains collagen fibers in pink-red. Right column: Toluidine Blue staining showing sulfated GAGs in purple. Original magnification 200×; scale bar: 100 µm.

In particular, a more intense collagen (Fig. 4 B, D) expression was observed in US-stimulated hMSCs compared to the non-US stimulated counterparts (Fig. 4 A, C); aggrecan was also detected in US-stimulated samples (data not shown), overall suggesting powerful US beneficial effects on matrix deposition, corroborating the findings of previous studies [18, 35, 37, 38]. Both elastic fibers (Fig. 4 A-F) and elastin (immunoistochemical reaction) could not be detected in these samples. The observation of larger and round shaped cells in 2D pre-differentiated hMSCs suggested the occurrence of some morphological changes compared to undifferentiated cells. A downregulation of type I collagen expression indicated an enhanced chondrogenic differentiation in US-stimulated samples, as previously observed by Barachini *et al.* [43]. The positivity levels of the expression of collagen and sulphated GAGs, as also shown in Fig. 4, are summarized in Table 3.

Table 3. Positivity levels of collagen and sulphated GAGs as observed via histochemistry under different culture conditions. − = negative; ∓ = weak positivity; + = positivity; ++ = good positivity; +++ = strong positivity.

Culture conditions	Total collagen	Sulphated GAGs
Miltenyi - US	∓	+
Miltenyi + US	+++	++
Home made − US	−	−
Home made + US	∓	−
Pellet + US	+	∓
2D + US	+	−

RT-PCR results showed a significantly higher collagen type II mRNA expression in US-stimulated constructs (130% ± 7% fold difference) than non-US stimulated constructs (100% ± 5% fold difference), therefore a more powerful chondrogenesis, in line with the results reported in literature [18, 37]. All in all, the constructs showed an intense cell colonization and ECM deposition, with a commitment to the chondrogenic phenotype, which was more pronounced using StemMACS ChondroDiff (Miltenyi) medium and US stimulation for 21 days.

However, these outcomes highlighted still an early chondrogenic phase, with weak production of collagen type II at protein level, good GAG synthesis but low aggrecan expression were observed.

Differently, synthesis of aggrecan, reduced collagen type I, increased collagen type II and even elastin was detected via immunohistochemistry on the cell/scaffold construct cultured within the bioreactor (Fig. 5), thus demonstrating that dynamic stimulation allows an improvement in chondrogenic differentiation of hMSCs with respect to static culture conditions. This bioreactor provides a cyclic membranal-like stress/deformation field that stretched the scaffolds and the cells cultured within. This outcome is suggestive that chondro-differentiated hMSCs can produce elastic fibers in presence of proper stimulation.

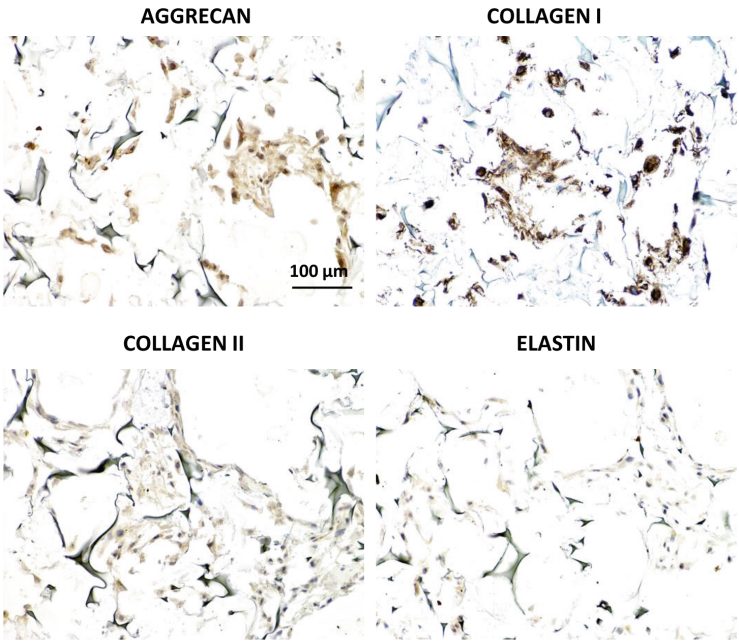

Fig. 5. Immunohistochemistry on chondroinduced hMSCs cultured on a PVA/G 70/30 (w/w)% scaffold in dynamic culture conditions using a bioreactor (WO/2015/040554): aggrecan, collagen type I, collagen type II, elastin. Original magnification: 200×; scale bar: 100 µm.

4 Conclusions

The aim of this work was the fabrication and characterization of bioartificial spongy scaffolds for the regeneration of auricular cartilage *in vitro* using bone marrow hMSCs. Morphological, physico-chemical and biomechanical characterization of PVA/G sponges demonstrated round-shaped interconnected pores, high swelling capacity, water stability and viscoelastic behavior. In particular, PVA/G 70/30 (w/w)% was selected for hMSC culture and chondrogenic lineage commitment, as this scaffold formulation presented higher G content, but similar morphological, physico-chemical and mechanical properties when compared to PVA/G 80/20 (w/w)%. *In vitro* studies were performed to identify the best chondrogenic differentiation conditions. Chondroinduced hMSCs were all over viable up to three weeks, thus proving scaffold cytocompatibility. StemMACS ChondroDiff commercially available medium positively affected cell metabolic activity and ECM deposition, thus appearing as the best differentiative medium. Histochemistry performed on cell/scaffold constructs proved intense sulphated GAG (but low aggrecan), glycoprotein and collagen synthesis after three weeks of differentiation. Immunohistochemistry for chondrogenic markers revealed an early differentiation stage, characterized by collagen type I and Sox-9. Since collagen type II was not detected at protein level, RT-PCR was used to assess its expression at gene level, revealing that mRNA was expressed both in non-US stimulated and US-stimulated constructs, with a 30% increase in the latter. US showed

beneficial effects on hMSC chondrogenesis in terms of enhancement of metabolic activity and type II collagen gene expression. Dynamic culture within a bioreactor finally proved an enhanced chondrogenic differentiation, by showing intense aggrecan, collagen type II and elastin expression at protein level. Further experiments are needed to investigate the combination of dynamic culture conditions and US to induce a mature cartilage ECM. Moreover, the used approach should also be scaled up to generate ear-shaped constructs of physiologically relevant dimensions by means of mold casting (Fig. 6). This study thus provided a basis for future development in this area.

Fig. 6. Example of a 1:2 size left auricle mold (2 cm × 3 cm) as obtained using reverse engineering and a Zortrax M200 3D printer.

Acknowledgements. AURICULAE Project, funded by Stem Cells & Life Foundation, Padova, Italy is greatly acknowledged. Dr. Delfo D'Alessandro (University of Pisa, Pisa, Italy), as well as Dr. Alessandra Fusco and Dr. Giovanna Donnarumma (University of Campania "Luigi Vanvitelli", Naples, Italy) are thanked for their fundamental technical support to this work.

References

1. Kamil, S.H., Vacanti, M.P., Vacanti, C.A., Eavey, R.D.: Microtia chondrocytes as a donor source for tissue-engineered cartilage. Laryngoscope **114**, 2187–2190 (2004)
2. Han, S.E., Lim, S.Y., Pyon, J.K., Bang, S.I., Mun, G.H., Oh, K.S.: Aesthetic auricular reconstruction with autologous rib cartilage grafts in adult microtia patients. J. Plast. Reconstr. Aesthetic Surg. **68**, 1085–1094 (2015)
3. Jessop, Z.M., Javed, M., Otto, I.A., Combellack, E.J., Morgan, S., Breugem, C.C., Archer, C.W., Khan, I.M., Lineaweaver, W.C., Kon, M., et al.: Combining regenerative medicine strategies to provide durable reconstructive options: auricular cartilage tissue engineering. Stem Cell Res. Ther. **7**, 19 (2016)
4. Griffin, M.F., Premakumar, Y., Seifalian, A.M., Szarko, M., Butler, P.E.M.: Biomechanical characterisation of the human auricular cartilages; implications for tissue engineering. Ann. Biomed. Eng. **44**, 3460–3467 (2016)

5. Thorne, C.H., Brecht, L.E., Bradley, J.P., Levine, J.P., Hammerschlag, P., Longaker, M.T.: Auricular reconstruction: Indications for autogenous and prosthetic techniques. Plastic Reconstr. Surg. **107**, 1241–1252 (2001)
6. Ciorba, A., Martini, A.: Tissue engineering and cartilage regeneration for auricular reconstruction. Int. J. Pediatr. Otorhinolaryngol. **70**, 1507–1515 (2006)
7. Cao, Y., Vacanti, J.P., Paige, K.T., Upton, J., Vacanti, C.A.: Transplantation of chondrocytes utilizing a polymer-cell construct to produce tissue-engineered cartilage in the shape of a human ear. Plastic Reconstr. Surg. **100**, 297–302 (1997)
8. Shieh, S.J., Terada, S., Vacanti, J.P.: Tissue engineering auricular reconstruction: in vitro and in vivo studies. Biomaterials **25**, 1545–1557 (2004)
9. Zhou, G., Jiang, H., Yin, Z., Liu, Y., Zhang, Q., Zhang, C., Pan, B., Zhou, J., Zhou, X., Sun, H., et al.: In vitro regeneration of patient-specific ear-shaped cartilage and its first clinical application for auricular reconstruction. EBioMedicine **28**, 287–302 (2018)
10. Schultz, T.W., Geneser, F.: Textbook of Histology. Transactions of the American Microscopical Society (1987)
11. Lai, C.H., Chen, S.C., Chiu, L.H., Yang, C.B., Tsai, Y.H., Zuo, C.S., Chang, W.H.S., Lai, W.F.: Effects of low-intensity pulsed ultrasound, dexamethasone/TGF-β1 and/or BMP-2 on the transcriptional expression of genes in human mesenchymal stem cells: chondrogenic vs. osteogenic differentiation. Ultrasound in Med. Biol. **36**, 1022–1033 (2010)
12. Murakami, W.T., Wong, L.W., Davidson, T.M.: Applications of the biomechanical behavior of cartilage to nasal septoplastic surgery. Laryngoscope **92**, 300–309 (1982)
13. Van Osch, G.J.V.M., Van Den Berg, W.B., Hunziker, E.B., Häuselmann, H.J.: Differential effects of IGF-1 and TGFβ-2 on the assembly of proteoglycans in pericellular and territorial matrix by cultured bovine articular chondrocytes. Osteoarthritis Cartilage **6**, 187–195 (1998)
14. Ackert, J.E., Maximow, A.A., Bloom, W.: A Textbook of Histology. Transactions of the American Microscopical Society (1942)
15. Gosline, J., Lillie, M., Carrington, E., Guerette, P., Ortlepp, C., Savage, K.: Elastic proteins: biological roles and mechanical properties. Philos. Trans. R. Soc. B: Biol. Sci. **357**, 121–132 (2002)
16. Lotz, M., Loeser, R.F.: Effects of aging on articular cartilage homeostasis. Bone **51**, 241–248 (2012)
17. Ross, M.H.P., Pawlina, W.: Histology a Text and Atlas with Correlated Cell and Molecular Biology (2014). ISBN 9780874216561
18. Xia, P., Wang, X., Qu, Y., Lin, Q., Cheng, K., Gao, M., Ren, S., Zhang, T., Li, X.: TGF-β1-induced chondrogenesis of bone marrow mesenchymal stem cells is promoted by low-intensity pulsed ultrasound through the integrin-mTOR signaling pathway. Stem Cell Res. Ther. **8**, 281–292 (2017)
19. Fung, Y.C., Skalak, R.: Biomechanics: Mechanical Properties of Living Tissues. Journal of Applied Mechanics (1982)
20. Urry, D.W., Hugel, T., Seitz, M., Gaub, H.E., Sheiba, L., Dea, J., Xu, J., Parker, T.: Elastin: a representative ideal protein elastomer. Philos. Trans. R. Soc. B: Biol. Sci. **357**, 169–184 (2002)
21. Milazzo, M., Jung, G.S., Danti, S., Buehler, M.J.: Wave propagation and energy dissipation in collagen molecules. ACS Biomater. Sci. Eng. **6**, 1367–1374 (2020)
22. Sherratt, M.J.: Tissue elasticity and the ageing elastic fibre. Age **31**, 305–325 (2009)
23. Nimeskern, L., Utomo, L., Lehtoviita, I., Fessel, G., Snedeker, J.G., van Osch, G.J.V.M., Müller, R., Stok, K.S.: Tissue composition regulates distinct viscoelastic responses in auricular and articular cartilage. J. Biomech. **49**, 344–352 (2016)

24. Riedler, K.L., Shokrani, A., Markarian, A., Fisher, L.M., Pepper, J.P.: Age-related histologic and biochemical changes in auricular and septal cartilage. Laryngoscope **127**, 399–407 (2017)
25. Vacanti, C.A., Vacanti, J.P.: Bone and cartilage reconstruction with tissue engineering approaches. Otolaryngol. Clin. North Am. **27**, 263–276 (1994)
26. Rodriguez, A., Cao, Y.L., Ibarra, C., Pap, S., Vacanti, M., Eavey, R.D., Vacanti, C.A.: Characteristics of cartilage engineered from human pediatric auricular cartilage. Plastic Reconstr. Surg. **103**, 1111–1119 (1999)
27. Otto, I.A., Levato, R., Webb, W.R., Khan, I.M., Breugem, C.C., Malda, J.: Progenitor cells in auricular cartilage demonstrate cartilage-forming capacity in 3D hydrogel culture. Eur. Cells Mater **35**, 132–150 (2018)
28. Ciuffreda, M.C., Malpasso, G., Musarò, P., Turco, V., Gnecchi, M.: Protocols for in vitro differentiation of human mesenchymal stem cells into osteogenic, chondrogenic and adipogenic lineages. In: Mesenchymal Stem Cells, pp. 149–158. Springer (2016)
29. Pittenger, M.F., Mackay, A.M., Beck, S.C., Jaiswal, R.K., Douglas, R., Mosca, J.D., Moorman, M.A., Simonetti, D.W., Craig, S., Marshak, D.R.: Multilineage potential of adult human mesenchymal stem cells. Science **284**, 143–147 (1999)
30. Kusuhara, H., Isogai, N., Enjo, M., Otani, H., Ikada, Y., Jacquet, R., Lowder, E., Landis, W.J.: Tissue engineering a model for the human ear: assessment of size, shape, morphology, and gene expression following seeding of different chondrocytes. Wound Repair Regener. **17**, 136–146 (2009)
31. Milazzo, M., Contessi Negrini, N., Scialla, S., Marelli, B., Farè, S., Danti, S., Buehler, M.J.: Additive manufacturing approaches for hydroxyapatite-reinforced composites. Adv. Funct. Mater. **29**, 1903055 (2019)
32. Cascone, M.G., Lazzeri, L., Sparvoli, E., Scatena, M., Serino, L.P., Danti, S.: Morphological evaluation of bioartificial hydrogels as potential tissue engineering scaffolds. J. Mater. Sci. Mater. Med. **15**, 1309–1313 (2004)
33. Moscato, S., Mattii, L., D'Alessandro, D., Cascone, M.G., Lazzeri, L., Serino, L.P., Dolfi, A., Bernardini, N.: Interaction of human gingival fibroblasts with PVA/gelatine sponges. Micron **39**, 569–579 (2008)
34. Kamoun, E.A., Chen, X., Mohy Eldin, M.S., Kenawy, E.R.S.: Crosslinked poly(vinyl alcohol) hydrogels for wound dressing applications: a review of remarkably blended polymers. Arab. J. Chem. **8**, 1–14 (2015)
35. Lee, H.J., Choi, B.H., Min, B.H., Son, Y.S., Park, S.R.: Low-intensity ultrasound stimulation enhances chondrogenic differentiation in alginate culture of mesenchymal stem cells. Artif. Organs **30**, 707–715 (2006)
36. Bernardo, M.E., Fibbe, W.E.: Mesenchymal stromal cells and hematopoietic stem cell transplantation. Immunol. Lett. **168**, 215–221 (2015)
37. Parvizi, J., Wu, C.C., Lewallen, D.G., Greenleaf, J.F., Bolander, M.E.: Low-intensity ultrasound stimulates proteoglycan synthesis in rat chondrocytes by increasing aggrecan gene expression. J. Orthop. Res. **17**, 488–494 (1999)
38. Jonnalagadda, U.S., Hill, M., Messaoudi, W., Cook, R.B., Oreffo, R.O.C., Glynne-Jones, P., Tare, R.S.: Acoustically modulated biomechanical stimulation for human cartilage tissue engineering. Lab Chip **18**, 473–485 (2018)
39. Aliabouzar, M., Lee, S.J., Zhou, X., Zhang, G.L., Sarkar, K.: Effects of scaffold microstructure and low intensity pulsed ultrasound on chondrogenic differentiation of human mesenchymal stem cells. Biotechnol. Bioeng. **115**, 495–506 (2018)
40. Ricci, C., Danti, S.: 3D models of pancreatic ductal adenocarcinoma via tissue engineering. Methods Mol. Biol. **1882**, 81–95 (2019)

41. Mattei, G., Tirella, A., Gallone, G., Ahluwalia, A.: Viscoelastic characterisation of pig liver in unconfined compression. J. Biomech. **47**, 2641–2646 (2014)
42. Tirella, A., Mattei, G., Ahluwalia, A.: Strain rate viscoelastic analysis of soft and highly hydrated biomaterials. J. Biomed. Mater. Res. - Part A **102**, 3352–3360 (2014)
43. Barachini, S., Danti, S., Pacini, S., D'Alessandro, D., Carnicelli, V., Trombi, L., Moscato, S., Mannari, C., Cei, S., Petrini, M.: Plasticity of human dental pulp stromal cells with bioengineering platforms: a versatile tool for regenerative medicine. Micron **67**, 155–168 (2014)
44. Bajpai, V.K., Mistriotis, P., Andreadis, S.T.: Clonal multipotency and effect of long-term in vitro expansion on differentiation potential of human hair follicle derived mesenchymal stem cells. Stem Cell Res. **8**, 74–84 (2012)
45. Gurikov, P., Smirnova, I.: Non-conventional methods for gelation of alginate. Gels **4**, 14 (2018)
46. De la Ossa, J.G., Trombi, L., D'Alessandro, D., Coltelli, M.B., Serino, L.P., Pini, R., Lazzeri, A., Petrini, M., Danti, S.: Pore size distribution and blend composition affect in vitro prevascularized bone matrix formation on poly(vinyl alcohol)/gelatin sponges. Macromol. Mater. Eng. **302**, 1700300 (2017)
47. Chiellini, E., Cinelli, P., Fernandes, E.G., Kenawy, E.R.S., Lazzeri, A.: Gelatin-based blends and composites. Morphological and thermal mechanical characterization. Biomacromol **2**, 806–811 (2001)
48. Bigi, A., Cojazzi, G., Panzavolta, S., Rubini, K., Roveri, N.: Mechanical and thermal properties of gelatin films at different degrees of glutaraldehyde crosslinking. Biomaterials **22**, 763–768 (2001)
49. Alves, P.M.A., Carvalho, R.A., Moraes, I.C.F., Luciano, C.G., Bittante, A.M.Q.B., Sobral, P.J.A.: Development of films based on blends of gelatin and poly(vinyl alcohol) cross linked with glutaraldehyde. Food Hydrocolloids **25**, 1751–1757 (2011)
50. Gao, X., Tang, K., Liu, J., Zheng, X., Zhang, Y.: Compatibility and properties of biodegradable blend films with gelatin and poly (vinyl alcohol). J. Wuhan Univ. Technol.-Mater. Sci. Ed. **29**, 351–356 (2014)
51. Pawde, S.M., Deshmukh, K.: Characterization of polyvinyl alcohol/gelatin blend hydrogel films for biomedical applications. J. Appl. Polym. Sci. **109**, 3431–3437 (2008)
52. Mattei, G., Gruca, G., Rijnveld, N., Ahluwalia, A.: The nano-epsilon dot method for strain rate viscoelastic characterisation of soft biomaterials by spherical nano-indentation. J. Mech. Behav. Biomed. Mater. **50**, 150–159 (2015)
53. Cacopardo, L., Mattei, G., Ahluwalia, A.: A new load-controlled testing method for viscoelastic characterisation through stress-rate measurements. Materialia **9**, 100552 (2020)